Taylor & Francis
Taylor & Francis Group

Fe(III) and cobalt(II) coordination compounds of 5-bromo-6-methyl-2-morpholinepyrimidinium-4-amine pyridine-2,6-dicarboxylate

HOSSEIN ESHTIAGH-HOSSEINI*, ZAKIEH YOUSEFI,
MARYAM SHAFIEE and MASOUD MIRZAEI

Department of Chemistry, School of Sciences, Ferdowsi University of
Mashhad, Mashhad 917791436, Iran

New coordination compounds, (bmmpaH)[Fe(pydc)$_2$]·(EtOH)$_{0.8}$(H$_2$O)$_{0.2}$ (**1**), (8QH) [Fe(pydc)$_2$]·H$_2$O (**2**), (2ampyH)$_2$[Mn(pydc)$_2$]·H$_2$O (**3**), (2ampyH)[Cr(pydc)$_2$](2ampy)$_{0.5}$·H$_2$O (**4**), [Co(H$_2$O)$_5$-μ-(pydc)Co(pydc)]·2H$_2$O (**5**), [Ni(pydcH)$_2$]·H$_2$O (**6**), and [Cu(pydcH)$_2$] (**7**), where bmmpa, 8Q, 2ampy, pydcH$_2$ are 5-bromo-6-methyl-2-morpholinepyrimidine-4-amine, 8-hydroxyquinoline, 2-amino-6-methylpyridine, and pyridine-2,6-dicarboxylic acid, respectively, have been synthesized and structurally characterized by elemental analyses, infrared, UV spectroscopic methods, and X-ray crystallography. Metal ions of **1** and **5** are six-coordinate with distorted octahedral geometries. Compound **1** is an anionic mononuclear complex and **5** is a binuclear compound constructed from cationic and anionic parts. The crystal data of **5** reveal that the cationic part is formed by five terminal waters and one μ-carboxylate oxygen O2 from the anionic portion and the anionic complex is built from two deprotonated (pydc)$^{2-}$ moieties. In the compounds, pydcH$_2$ is tridentate by one nitrogen of pyridine ring and two oxygens of carboxylate.

Keywords: Proton transfer compound; Pyridine-2,6-dicarboxylic acid; 5-Bromo-6-methyl-2-morpholinepyrimidine-4-amine; 2-Aminopyridine; Crystal structure

1. Introduction

Aromatic multi-carboxylic acids have predictable and interesting supramolecular properties and capability of forming hydrogen bonds. Pyridinedicarboxylic acids (PDAs) as assembler ligands or proton donating in proton transfer methodology have been increasingly used [1–10]. It should be noted that PDAs are present in many natural products, such as alkaloids, vitamins, and co-enzymes, so their metal complexes can be used as models in many research fields, especially in food chemistry [11]. Many researchers have designed PDA derivatives to tune their coordination ability and biological activity. For instance, 1 : 1 complex of Ca^{2+}–pydc^{2-} is important in spore resistance to many environmental stresses and in spore stability [12]. The (pydc)$^{2-}$ possesses a variety of bonding abilities and exhibits strong hydrogen bonds during

---

*Corresponding author. Email: heshtiagh@um.ac.ir

complexation with metal ions [13]. For further understanding of coordination modes of $(\text{pydc})^{2-}$ and as a continuation of previously reported works [14–16], we applied pydcH$_2$ along with bmmpa, 8Q, and 2ampy moieties in reactions with first row metals from IVB to IB groups. Herein, pydcH$_2$ is a tridentate ligand by one nitrogen of pyridine and two oxygens of carboxylates. The obtained data from X-ray crystallography show that **1** contains a six-coordinate complex of Fe(III) with protonated bmmpa and **5** is a binuclear complex of Co(II). Indeed, the bridging role of the carboxylic group in **5** leads to a neutral complex. As an interesting feature, the bmmpa organic base in discrete form is not soluble in water, but it is fully soluble in water in its counter-ionic form in crystalline network of the synthesized coordination compound.

2. Experimental

2.1. *Material and instruments*

The bmmpa was synthesized according to scheme 1. Other reagents and chemicals were purchased from commercial sources and used as received. Infrared (IR) spectra from 4000 to 600 cm^{-1} were recorded on a Buck 500 scientific spectrometer using KBr discs. UV spectra were obtained on an Agilent 8453 single-beam photodiode-array
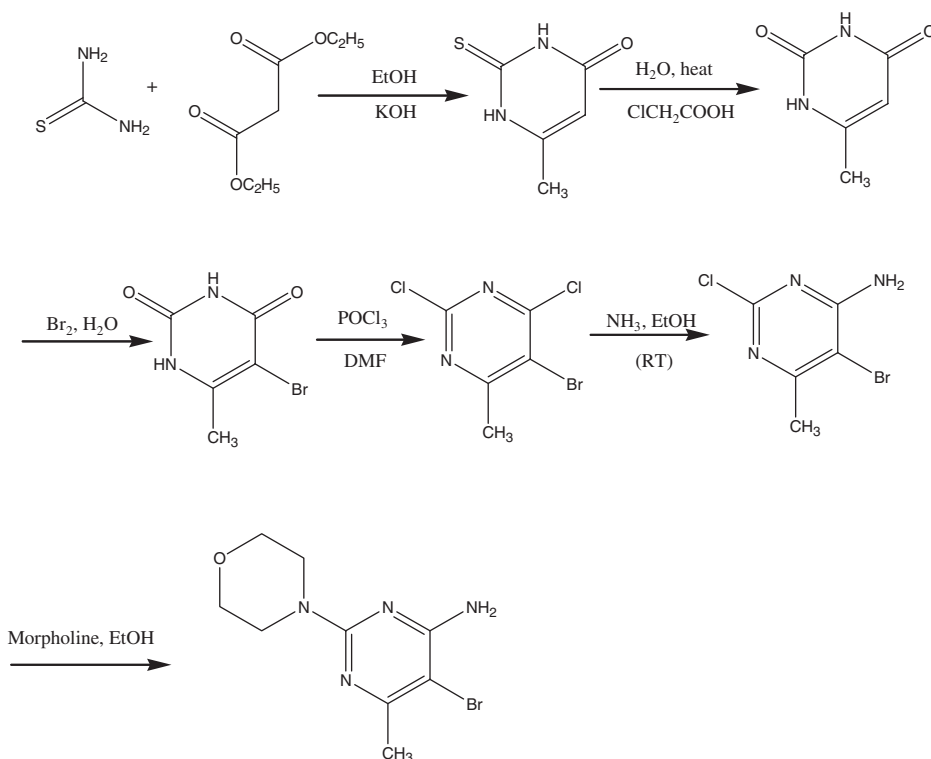
Scheme 1.   Synthetic path of bmmpa.

spectrometer from 190 to 700 nm. Elemental analyses were carried out with a Thermo Finnigan Flash-1112EA microanalyzer. Except for C, H, and N atoms, which were measured by microanalyzer, the elements were measured by ICP method. The X-ray diffraction data were collected with a Bruker SMART CCD diffractometer. Melting points were determined using an Electro thermal IA-9100 apparatus and are not corrected.

2.2. Synthesis of 1

A solution of $Fe(NO_3)_3 \cdot 9H_2O$ (0.073 g, 0.180 mmol) in ethanol (5 mL) was added to a solution of pydcH$_2$ (0.060 g, 0.36 mmol) and bmmpa (0.05 g, 0.180 mmol) in ethanol (5 mL) in 1 : 2 : 1 molar ratio. The resulting solution was refluxed at 50°C for 3 h. After one day, by slow evaporation at room temperature, light green crystals suitable for X-ray measurements were obtained (yield 30%, m.p. >300°C). Anal. Calcd for $C_{24.60}H_{25.20}BrFeN_6O_{10}$ (%): C, 42.16; H, 3.59; N, 11.99; Fe, 7.97; Br, 11.40. Found (%): C, 39.83; H, 3.34; N, 11.71; Fe, 7.65; Br, 10.73. IR (KBr, cm^{-1}): 3500–3000(br), 1780(m), 1760(m), 1720(m), 1340(m), 1280(w), 1180(w), 1120(w), 1080(w), 1040(w), 920(w), 880(w), 780(w), 740(m), 680(m). UV (H$_2$O): $\lambda(\varepsilon, 10^5)$: 220(0.13), 250(0.087), 275(0.0436), 300(0.0264).

2.3. Synthesis of 5

To 0.177 g (1.062 mmol) of pydcH$_2$ and 0.050 g (0.531 mmol) of 2-aminopyridine in 8 mL of water, an aqueous solution containing 0.132 g (0.531 mmol) of $Co(OAc)_2 \cdot 4H_2O$ was added dropwise. The latter mixture was stirred for 4 h at 70°C. By slow evaporation at room temperature, dark red crystals of the title compound suitable for X-ray measurements were isolated after 28 days (yield 25%, m.p. 221°C). Anal. Calcd for $C_{14}H_{20}Co_2N_2O_{15}$ (%): C, 29.30; H, 3.51; N, 4.88, Co, 20.52. Found (%): C, 29.27; H, 3.50; N, 4.85; Co, 20.00. IR (KBr, cm^{-1}): 3372(br), 3220(br), 3106(br), 1730(s), 1642(vs), 1650-1550(vs, br), 1440(m), 1388(s), 767(m), 723(m), 682(m). UV (H$_2$O): $\lambda(\varepsilon, 10^5)$: 267(4.20).

2.4. Crystal structure determination and refinement

Suitable crystals of **1** and **5** for X-ray diffraction were grown by slow evaporation of solvents at room temperature. X-ray diffraction experiments were carried out on a Bruker SMART diffractometer with an APEX II CCD area detector (Mo-Kα radiation, graphite monochromator, $\lambda = 0.71073$ Å). Diffracted data were corrected for absorption using SADABS. Some software including APEX II (data collection), SAINT$^+$ (cell refinement and data reduction), and SHELXTL (version 6.2, structure solution and refinement; molecular graphics and publication material) were used [17, 18].
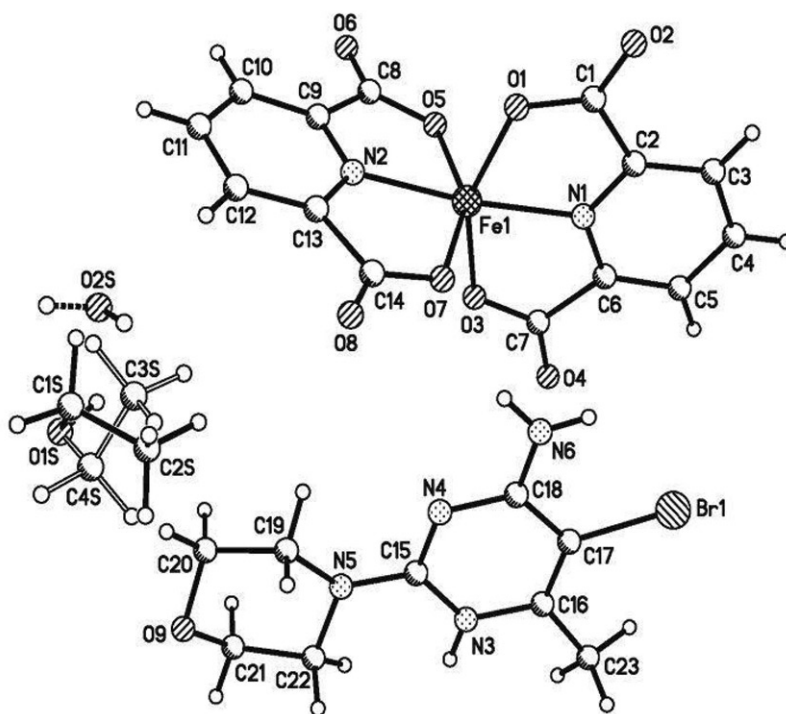
Figure 1.　Molecular structure of **1**; ellipsoids are shown at 50% probability.

3. Results and discussion

3.1. *Description of molecular structures of 1 and 5*

3.1.1. Structure of (bmmpaH)[Fe(pydc)$_2$] · (EtOH)$_{0.8}$(H$_2$O)$_{0.2}$ (1). The numbering scheme of non-hydrogen atoms along with the thermal vibrational ellipsoids of **1** are shown in figure 1. A summary of parameters for the data collection and refinements is given in table 1. Selected bond distances, bond and torsion angles are given in table 2. In addition, a list of hydrogen bonds is given in table 3. In the asymmetric unit, the molecular structure of **1** contains [Fe(pydc)$_2$]$^-$, bmmpaH$^+$, ethanol, and water in $1 : 1 : 0.8 : 0.2$ molar ratios, respectively. The [Fe(pydc)$_2$]$^-$ anion has a significantly distorted octahedral coordination formed by two tridentate (pydc)$^{2-}$ ligands (figure 1). Most of the bond lengths and angles (table 2) are comparable to those reported for [Fe(bpy)$_3$][Fe(pydc)$_2$]$_2$ · (pydcH$_2$)$_{1/2}$ · 6.5H$_2$O [19]. The mean bond length of Fe–O is ~2.0221 Å, similar to those previously reported [19]. In our recent studies on the coordination behavior of pydcH$_2$ and its ability in proton donation to different bases, we synthesized (2-apym)[Cr(pydc)$_2$] · 2H$_2$O (2-apym is 2-aminopyrimidine) [20] in which bond lengths and angles are comparable with **1**. On the basis of torsion angles in the anionic complex, the planes of tridentate ligands are quasi-perpendicular to each other. Intermolecular forces between the anionic and cationic units in this complex consist of hydrogen bonding, $\pi \cdots \pi$ stacking, and ion pairing. The most important is C$-$H$\cdots \pi$

Table 1. Crystal data and structure refinement parameters for **1** and **5**.

Compound	**1**	**5**
Empirical formula	$C_{24.60}H_{25.20}BrFeN_6O_{10}$	$C_{14}H_{20}Co_2N_2O_{15}$
Formula weight	700.67	574.18
Temperature (K)	120(2)	120(2)
Wavelength (Å)	0.71073	0.71073
Crystal system	Triclinic	Monoclinic
Space group	$P\bar{1}$	$P2_1/c$
Unit cell dimensions (Å, °)		
a	8.9305(6)	8.3597(5)
b	13.0051(9)	27.1800(16)
c	13.2143(2)	9.5926(6)
α	110.6290(10)	90.00
β	102.4070(10)	98.1270(10)
γ	93.6120(10)	90.00
Z	2	4
Absorption coefficient (mm^{-1})	2.053	1.617
Crystal size (mm^3)	$0.55 \times 0.40 \times 0.12$	$0.33 \times 0.30 \times 0.29$
Calculated density ($Mg\,m^{-3}$)	1.678	1.768
$F(000)$	712	1168
θ range for data collection	1.69–28.00	2.27–28.99
Index ranges	$-11 \leq h \leq 11$,	$-11 \leq h \leq 11$,
	$-17 \leq k \leq 17$,	$-37 \leq k \leq 37$,
	$-17 \leq l \leq 17$	$-13 \leq l \leq 13$
Reflections collected	14,313/6659	31,547/5730
	$[R(int) = 0.0224]$	$[R(int) = 0.0332]$
Refinement method	Full-matrix least-squares on F^2	Full-matrix least-squares on F^2
Data/restraints/parameters	6659/0/413	5730/0/298
Final R indices $[I > 2\sigma(I)]$	$R_1 = 0.0293$,	$R_1 = 0.0326$,
	$wR_2 = 0.0807$	$wR_2 = 0.0661$
Largest difference peak and hole ($e\,Å^{-3}$)	0.552 and -0.464	1.113 and -0.45

Table 2. Selected bond lengths and angles for **1** and **5**.

(bmmpaH)[Fe(pydc)$_2$] · (EtOH)$_{0.8}$(H$_2$O)$_{0.2}$ (**1**)			
Fe1–O3	2.0346(12)	Fe1–N1	2.0578(14)
Fe1–O1	2.0203(12)	Fe1–N2	2.0612(14)
Fe1–O5	2.0157(12)	N2–Fe1–O5	76.09(5)
Fe1–O7	2.0179(12)	N2–Fe1–O7	75.98(5)
N1–Fe1–N2	173.726(94)	O5–Fe1–O7	151.54(5)
N1–Fe1–O3	75.94(5)	O1–Fe1–O7–C14	89.50(13)
N1–Fe1–O1	76.00(5)	O1–Fe1–O5–C8	$-91.38(12)$
O1–Fe1–O3	151.94(5)		

[Co(H$_2$O)$_5$-μ-(pydc)Co(pydc)] · 2H$_2$O (**5**)			
Co2–O1 W	2.0542(15)	Co1–O4	2.1801(14)
Co2–O2 W	2.0522(16)	Co1–O5	2.1135(15)
Co2–O3 W	2.1690(15)	Co1–O8	2.1730(15)
Co2–O4 W	2.0851(15)	Co1–N1	2.0257(17)
Co2–O5 W	2.0872(15)	Co1–N2	2.01661(17)
Co2–O2	2.0912(14)	O2–C1	1.248(2)
Co1–O1	2.2153(14)	O6–C8	1.247(3)
O2–Co2–O1 W	79.78(6)	O1–Co1–O8	96.85(6)
O2–Co2–O2 W	87.09(6)	O1–Co1–O5	97.38(6)
O2–Co2–O3 W	95.53(6)	O1–Co1–N1	76.19(6)
O2–Co2–O4 W	90.39(6)	O8–Co1–O5	149.87(6)
O2–Co2–O5 W	170.49(6)	O4–Co1–N1	75.58(6)
O1 W–Co2–O4 W	168.69(6)	O8–Co1–N2	75.72(6)
O2 W–Co2–O3 W	176.58(6)	O5–Co1–N2	76.52(6)
Co2–O2–C1	132.75(14)	N1–Co2–N2	171.95(7)

Table 3.　Hydrogen bonds for **1** and **5**.

D–H⋯A	d(D–H)	d(H⋯A)	d(D⋯A)	∠(DHA)
(bmmpaH)[Fe(pydc)$_2$]·(EtOH)$_{0.8}$(H$_2$O)$_{0.2}$ (**1**)				
N(3)–H(1N3)⋯O(4)#1	0.9	1.99	2.870(2)	167
N(6)–H(1N6)⋯Br(1)	0.85	2.72	3.094(2)	108
N(6)–H(1N6)⋯O(2)#2	0.85	2.09	2.808(2)	142
N(6)–H(2N6)⋯O(7)	0.85	2.12	2.918(2)	156
O(1 S)–H(1SO)⋯O(6)#3	0.85	2.02	2.853(2)	166
[Co(H$_2$O)$_5$-μ-(pydc)Co(pydc)]·2H$_2$O (**5**)				
O(1 W)–H(1WA)⋯O(3)#1	0.85	1.79	2.637(2)	174
O(1 W)–H(1WB)⋯O(6 W)	0.85	2.17	2.943(2)	152
O(2 W)–H(2WA)⋯O(6)#2	0.85	1.87	2.715(2)	172
O(2 W)–H(2WB)⋯O(6 W)#3	0.85	1.98	2.821(2)	169
O(3 W)–H(3WA)⋯O(3)#4	0.85	1.83	2.6755(19)	171
O(3 W)–H(3WB)⋯O(8)#5	0.85	1.97	2.787(2)	159
O(4 W)–H(4WA)⋯O(7)#5	0.85	1.86	2.698(2)	169
O(4 W)–H(4WB)⋯O(1)	0.85	1.98	2.818(2)	168
O(5 W)–H(5WA)⋯O(4)#1	0.85	1.93	2.764(2)	167
O(5 W)–H(5WB)⋯O(7 W)#2	0.85	1.81	2.654(2)	175
O(6 W)–H(6WA)⋯O(3 W)#6	0.85	2.06	2.898(2)	169
O(6 W)–H(6WB)⋯O(5)#4	0.85	2.22	3.016(2)	156
O(7 W)–H(7WA)⋯O(7)#7	0.85	1.93	2.775(2)	174
O(7 W)–H(7WB)⋯O(6)	0.85	1.96	2.767(2)	158

Symmetry codes for **1**: #1: $-x$, $-y+1$, $-z+1$; #2: $-x+1$, $-y$, $-z+1$; #3: $-x$, $-y$, $-z$; for **5**: #1: $x-1$, y, $z-1$; #2: x, y, $z-1$; #3: $-x+1$, $-y+1$, $-z$; #4: $-x+1$, $-y+1$, $-z+1$; #5: $x-1$, y, z #6: $-x$, $-y+1$, $-z$ #7: $x-1$, $-y+3/2$, $z+\frac{1}{2}$.

interaction at 3.483 Å (figure 2), formed between hydrogen of ethanol and π-electrons of pyridine of (pydc)$^{2-}$. Figure 3 shows the packing diagram of **1**. By considering this pattern, we can conclude that this compound contains a layer structure formed by anionic complex connected *via* H-bonds. The arrangement of these layers makes space for organic molecules.

3.1.2. Structure of [Co(H$_2$O)$_5$-μ-(pydc)Co(pydc)] · 2H$_2$O (5).

The numbering scheme of the non-hydrogen atoms along with the thermal vibrational ellipsoids of **5** are shown in figure 4. A summary of parameters for data collection and refinement is given in table 1. Selected bond distances, angles, and torsion angles are given in table 2 and a list of hydrogen bonds in table 3. In the asymmetric unit the molecular structure of **5** contains [Co(H$_2$O)$_5$-μ-(pydc)Co(pydc)], a binuclear Co(II) complex which exhibits an extended hydrogen bonding network. The coordination environment around Co(II) is distorted octahedral (figure 4) with the cationic portion of **5** a centrosymmetric complex with the center of inversion lying on Co(2). There are two crystallographically independent Co(II)'s. Compound **5** consists of asymmetric dimeric units with independent Co(1)/Co(2) centers. The cationic part is formed by a six-coordinate Co(2) with distorted octahedral geometry filled by five terminal waters and one μ-carboxylate O2 from the anionic portion of the compound. The anionic moiety comprises a distorted octahedral Co(1) with two deprotonated carboxylate moieties as tridentate chelates. The binding of (pydc)$^{2-}$ involves the five-membered chelate rings as Co1–O1–C1–C2–N1, Co1–O4–C7–C6–N1, Co1–O8–C14–C13–N2, and Co1–O5–C8–C9–N2 with O–Co–N bite angles of 76.19(6), 75.58(6), 75.72(6), and 76.52(6) Å,
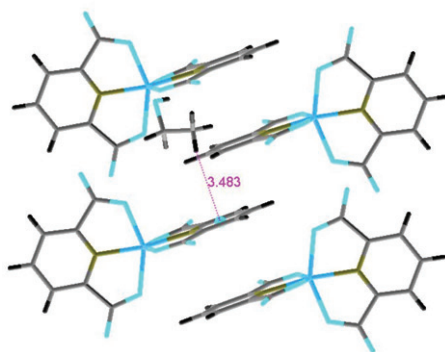
Figure 2.   Schematic representation of C−H···π interaction in **1**.
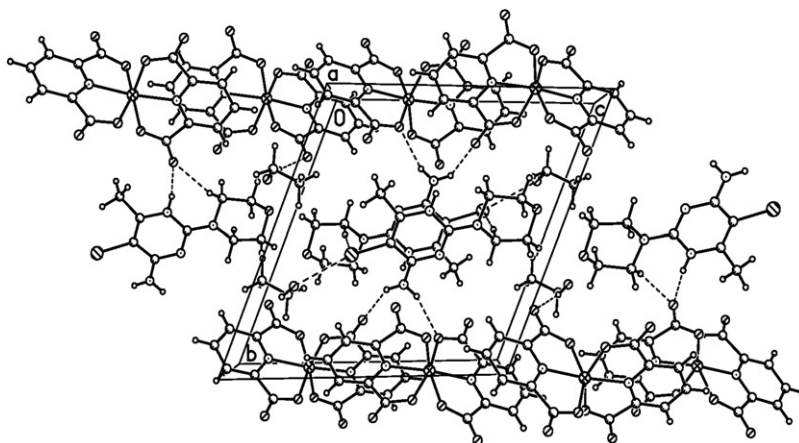

Figure 3.   Packing diagram of **1**. Dashed lines are hydrogen bonds.

respectively, reduced significantly from the expected octahedral 90° (figure 4). The distortion around Co(1) reflects in Co–O bond distances which vary from 2.2153(14) to 2.1135(15) Å for Co1–O1 and Co1–O5, respectively. A slight deviation in the Co–O distances between two carboxylates (average: 0.054 Å) is observed in **5**. The $[Co(H_2O)_5]^{2+}$ unit is less distorted from ideal in comparison with $[Co(pydc)_2]^{2-}$. The length of the Co2–O2 bond (2.0912 Å) which combines cationic and anionic parts of compound is equal to the average Co–OH$_2$ bond length of 2.08954 Å calculated from Co2–O1w, Co2–O2w, Co2–O3w, Co2–O4w, and Co–O5w bond distances. The connection of the cationic and anionic parts of **5** is additionally stabilized by an intramolecular O4w–H4w···O1 hydrogen bond of *ca* 1.9800 Å between one coordinated water and one carboxylate oxygen forming a chelating Co2–O4w···O1–C1–O2 ring with O4w–Co2–O2 bite angle of 90.39(6)°. Extensive intra- and inter-molecular O–H···O hydrogen bonds are also formed by coordinated (O1w–O5w) and two crystallization waters (O6w and O7w) and carboxylate oxygens stabilizing the crystalline network. In summary, Co(1) is equatorially coordinated to two (pydc)$^{2-}$
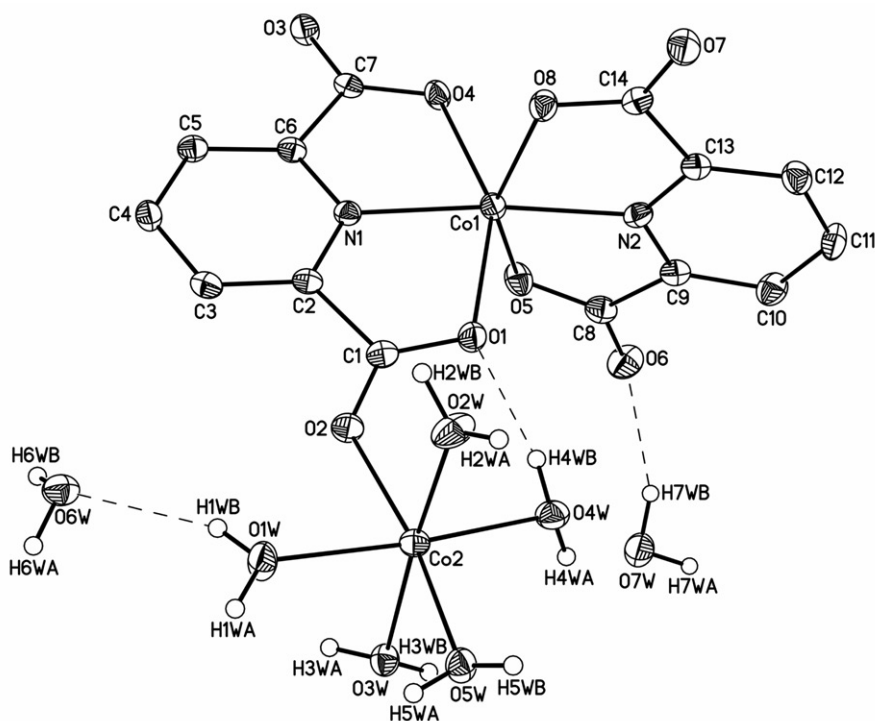
Figure 4. Molecular structure of **5**; ellipsoids are shown at 50% probability. Dashed lines are hydrogen bonds.

through two nitrogens and four oxygens. As can be seen from the packing diagram of **5** (figure 5), there is hydrogen bonding in the crystal lattice (table 3) that stabilizes the crystal packing.

3.2. Spectroscopic characterization

3.2.1. IR spectroscopy. IR spectra of complexes containing pydcH$_2$ have characteristic absorption bands. The main IR spectral data are given in table 4. The most definitive feature in **1** is the presence of asymmetric and symmetric carboxylate stretching frequencies at 1600 and 1340 cm^{-1}, respectively [11]. The separation between $\nu_{as}(COO^-)$ and $\nu_s(COO^-)$ has often been used to diagnose coordination modes [21] with unidentate carboxylate >200 and <200 cm^{-1} for bidentate. Thus, the separation of 260 cm^{-1} in the Fe(III) complex indicates a unidentate coordination mode. The δ(O–C–O) in plane deformation vibration of (pydc)$^{2-}$ ring occurs at 740 cm^{-1} and wagging vibrations of rings are located at 680 and 740 cm^{-1} [13]. The band at 3100 cm^{-1} is due to C–H stretching vibration and stretching frequency of pyrimidine is 920 cm^{-1}. The observed IR bands for **2–7** are similar to the reported bands for **1**. The similarity of IR
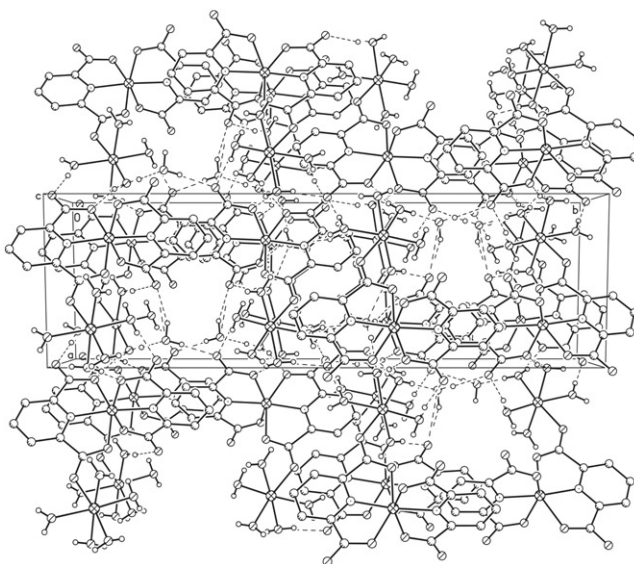
Figure 5.   Packing diagram of **5**. Dashed lines are hydrogen bonds.

data and elemental analyses for **6** and **7** may support these compounds being isomorphic.

3.2.2. UV spectra.   The UV spectrum of **1** involved bands at 200, 250, 275, and 300 nm which may be attributed to $n \rightarrow \pi^*$, interligand transfer of bmmpa, $\pi \rightarrow \pi^*$, and charge transfer transitions, respectively. The electronic absorption spectrum of **5** in aqueous solution exhibits a band at 267 nm in the UV region which is assigned to a $\pi–\pi^*$ transition [22].

4. Conclusion

For better understanding of coordination modes of pydcH$_2$ in the presence of organic spacers, we synthesized and structurally characterized seven complexes based upon pydcH$_2$ ligand. Different interactions resulting from ion-pairing, C−H$\cdots\pi$ and $\pi\cdots\pi$ stacking interactions, and hydrogen bonding play essential roles in the construction of 3-D layered networks of **1** and **5**. Indeed, in all of these synthesized complexes, pydcH$_2$ is tridentate. All prepared compounds were characterized by some physico-chemical approaches for determining their chemical formula. The obtained results (melting point, elemental analyses, IR, ICP, and UV) for compounds **2**–**4**, **6**, and **7** are gathered in table 4. Many aspects of these coordination compounds, such as single crystal X-ray structure determination and biological studies, remain to be investigated as we intend to do in the near future.

Table 4. Obtained characterization data for **1–7**.

Compound	Melting point (°C)	Molar ratio Acid:base:metal	ICP/C.H.N Found (Anal. Calcd) %			UV (nm)	IR (cm⁻¹)					
			C	H	N		ν_{as} (COO⁻)	ν_s (COO⁻)	$\Delta\nu$	δ (O–C–O)	C=C	C=N
1	>300	2:1:1	39.83 (42.16)	3.34 (3.59) Fe 7.65 (7.97)	11.71 (11.99) Br 10.73 (11.40)		1600	1340	260	740		
2	270	2:1:1	52.66 (50.21)	2.82 (2.93) Fe 10.02(10.15)	7.75 (7.67)	243: $\pi \rightarrow \pi^*$ in pyridine 601, 619, 648	1664	1322	342	753	1410	1557
3	200	2:2:1	53.58 (51.75)	4.25 (4.01) Mn 8.51(8.84)	14.04 (13.93)	226: $n \rightarrow \pi^*$ of pyridine 277: $\pi \rightarrow \pi^*$ in pyridine 305: charge transfer	1673	1381	292	773	1422	1577
4	>300	2:1:1	49.44 (48.98)	3.72 (3.73) Cr 8.76(9.23)	12.86 (12.42)	226: $n \rightarrow \pi^*$ of pyridine 266: $\pi \rightarrow \pi^*$ in pyridine 304: charge transfer 553: $d \rightarrow d$ transition	1682	1332	350	742	1456	1484
5	221	2:1:1	29.30 (29.27)	3.51 (3.50) Co 20.00(20.52) Ni 12.74(13.19)	4.88 (4.85)	267: $\pi \rightarrow \pi^*$ in pyridine	1600	1380	220	723	1550	1617
6	>300	2:2:1	41.12 (40.95)	2.46 (2.42) Ni 13.56(14.35)	6.85 (6.74)	263, 270: $\pi \rightarrow \pi^*$ in pyridine	1600	1350	250	690	1452	1601
7	>300	2:2:1	42.49 (42.83)	2.04 (2.05) Ni 16.00(16.05)	7.08 (6.78)	269, 277: $\pi \rightarrow \pi^*$ in pyridine	1638	1381	257	686	1451	1601

Supplementary material

Crystallographic data for these two structures have been deposited with the Cambridge Crystallographic Data Center, CCDC 752206 for **1** and CCDC 730752 for **5**. Copies of the data can be obtained free of charge on application to the Director, CCDC, 12 Union Road, Cambridge CB2 1EZ, UK (Fax: int. code +(1223)336-033; Email for inquiry: fileserv@ccdc.cam.ac.uk; Email for deposition: deposit@ccdc.cam.ac.uk).

Acknowledgment

References

[1] J.R. Li, Y. Tao, X.H. Bu. *Cryst. Growth Des.*, **6**, 2493 (2006).
[2] H. Aghabozorg, F. Manteghi, S. Sheshmani. *J. Iran. Chem. Soc.*, **5**, 184 (2008).
[3] B. Masci, P. Thuery. *Cryst. Growth Des.*, **8**, 1689 (2008).
[4] H. Aghabozorg, M. Ghdermazi, J. Attar Gharamaleki. *Anal. Sci.*, **23**, x209 (2007).
[5] W. Starosta, H. Ptasiewicz-Bak, J. Leciejewicz. *J. Coord. Chem.*, **55**, 873 (2002).
[6] X. Hu, Y. Li, Y. Wang, W. Du, J. Guo. *J. Coord. Chem.*, **62**, 3438 (2009).
[7] H. Aghabozorg, F. Manteghi, M. Ghadermazi, M. Mirzaei, A.R. Salimi, H. Eshtiagh-Hosseini. *J. Iran. Chem. Soc.*, **2** (2010).
[8] C.-Z. Xie, B. Yu, X.-Q. Wang, R.-J. Wang, G.-Q. Shen, D.-Z. Shen. *J. Coord. Chem.*, **59**, 2005 (2006).
[9] H. Aghabozorg, E. Motyeian, R. Khadivi, M. Ghadermazi, F. Manteghi. *Acta Cryst.*, **E64**, m320 (2008).
[10] H. Aghabozorg, R. Khadivi, M. Ghadermazi, H. Pasdar, S. Hooshmand. *Acta Cryst.*, **E64**, m267 (2008).
[11] H. Aghabozorg, M. Ghadermazi, B. Nakhjavan, F. Manteghi. *J. Chem. Crystallogr.*, **38**, 135 (2008).
[12] S.-S. Huang, D. Chen, P.L. Pelczar, V.R. Vepachedu, P. Setlow, Y.-Q. Li. *J. Bacteriol.*, **189**, 4681 (2007).
[13] A.T. Colak, O.Z. Yesilel, T. Hôkelek, E. Sahin. *Struct. Chem.*, **19**, 285 (2008).
[14] M. Ranjbar, A. Moghimi, H. Aghabozorg, G.P.A. Yap. *Anal. Sci.*, **18**, 219 (2002).
[15] F. Ramezanipour, H. Aghabozorg, A. Shokrollahi, M. Shamsipur, H. Stoeckli-Evans, J. Soleimannejad, S. Sheshmani. *J. Mol. Struct.*, **779**, 77 (2005).
[16] H. Aghabozorg, F. Manteghi, M. Ghadermazi, M. Mirzaei, A.R. Salimi, A. Shokrollahi, S. Derki, H. Eshtiagh-Hosseini. *J. Mol. Struct.*, **919**, 381 (2009).
[17] Bruker. *SAINT⁺ (Version 6.2), Data Reduction and Correction Program*, Bruker AXS, Madison, Wisconsin, USA (2001).
[18] (a) G.M. Sheldrick. *SHELXTL (Version 6.12), Structure Determination Software Suite*, Bruker AXS, Madison, Wisconsin, USA (2001). (b) Bruker. *APEX II Software Package (Version 1.27). Bruker Molecular Analysis Research Tool*, Bruker AXS, Madison, Wisconsin, USA (2005).
[19] H. Aghabozorg, F. Mohammad Panah, E. Sadr-Khanlou. *Anal. Sci.*, **23**, x139 (2007).
[20] H. Eshtiagh-Hosseini, Z. Yousefi, M. Mirzaei, Y.-G. Chen, S.A. Beyramabadi, A. Shokrollahi, R. Aghaei. *J. Mol. Struct.*, **973**, 1 (2010).
[21] I. Ucar, B. Karabulut, A. Bulut, O. Büyükgüngör. *J. Mol. Struct.*, **834–836**, 336 (2007).
[22] L. Wasylina, E. Kucharska, Z. Weglinski, A. Puszko. *Chem. Heterocycl. Comp.*, **35**, 186 (1999).